Journal of Building Pathology and Rehabilitation (2022) 7:85
https://doi.org/10.1007/s41024-022-00224-8

RESEARCH ARTICLE

Experimental investigation on bond behaviour, durability and microstructural analysis of self-compacting concrete using waste copper slag

Bypaneni Krishna Chaitanya[1,2] · **Ilango Sivakumar**[1]

Received: 7 May 2022 / Revised: 17 July 2022 / Accepted: 19 July 2022 / Published online: 8 August 2022

Abstract
This study will investigate the viability of SCC constructed using fine aggregates derived from waste copper slag (WCS). WCS replacement ranged from 0 to 70% (10% increments) with sand at constant W/C ratio of 0.43; eight SCC mixtures were prepared. The cement content was substituted with 17.85% fly ash (FA), and a consistent amount of superplasticizer was utilized for the experiment. Tests on SCC mixes included mechanical properties like compressive strength at 28, and 56 days, pull-out tests after 28 days of curing, and durability tests, including rapid chloride permeability test (RCPT), and water absorption, and sorptivity after 28 days of curing were tested. Results showed that maximum compressive strength was noticed for 40% WCS. In the pull-out test, the maximum pull-out load and bond stress are recorded at 40% and 50% WCS is 44.35kN, 44.3kN and 11.76 MPa, 11.54 MPa compared to the control concrete mix (WCS0%). In terms of longevity, there is a strong link between CMS and several other performance metrics. Scanning electron microscopy, XRD analysis, and energy dispersive spectroscopy were used to analyze the microstructure of concrete. WCS may be used as a substitute for fine aggregates in concrete up to 70% which can benefit the building industry. By using this method, copper slag may be safely disposed of without damaging the environment or requiring land management.

Keywords Microstructure · Compressive strength · Waste copper slag · Chloride permeability · Water absorption · Sorptivity

1 Introduction

After agriculture, building is the second-largest economic sector in India [1–3]. In the building sector, concrete play a major role in faster construction. In concrete, self-compacting concrete (SCC) play a vital role due to its flow and compaction under its weight. These are distinctive properties of SCC, which was created in 1988 and initially used in the construction industry [4–7]. There is no need for external vibration for the SCC process. Natural resource conservation in the current and future is a difficult task for the construction industry. Rather than being a consumable sector, the building industry must now become sustainable. The estimated production of building aggregates worldwide in 2015 was around 48.3 billion tonnes. About 70% of the volume of concrete is accounted for by aggregates [8]. Nearly 2.2–3 tonnes of slag are generated for each tonne of copper produced (source). Large amounts of copper slag are often dumped in landfills, causing pollution to the environment. A solution that is technically sound, environmentally friendly, and economically sound may be found in the use of waste copper slag (WCS) as a fine aggregate in SCC. Concrete's resistance to chemical, biological, and physical disintegration might be considered its durability. The use of CS as fine aggregates in the creation of SCC is a unique aspect of the study. When it comes to building infrastructure, natural resources are always in short supply. The WCS can help alleviate that problem. The primary goal of this research is to use WCS to accomplish concrete's durability performance at a level that is equivalent to or better than concrete. Rajasekar et al. [1] UHSC with a compressive strength of moreover 150 MPa

✉ Bypaneni Krishna Chaitanya
krishnachtn945@gmail.com

[1] Civil and Structural Engineering Department, Annamalai University, Chidambaram, Tamilnadu, India

[2] Civil Engineering Department, R.V.R & J.C College of Engineering (A), Guntur, Andhra Pradesh, India

may be made utilizing untreated copper slag and treated copper slag as quartz sand, according to test results. The 30 CS-UHSC was shown to be more durable than a control quartz sand UHSC. Copper slag may be used for quartz sand in the production of UHSC [1]. Sharma and Khan [8] the minimal carbonation depth was found by substituting 100% CS and 10% MK for FA The experiment's outcomes. CS with 10% MK had lower initial surface absorption and sorptivity than control concrete during curing [8]. Gupta and Siddique [9] copper slag replaced natural sand, boosting strength by 10%. SCC durability was determined by water absorption, chloride permeability, and sorptivity. As long as the SCC mix included no more than 30% copper slag, the results were almost equal to a control mix [9]. Sharma and Khan [10] using six SCC combinations, a constant w/b ratio of 0.45, the copper slag was replaced by the SCC. When exposed to sulphate, concrete mixtures lose compressive strength while gaining weight. Reduced carbonation is one potential benefit of making steel from copper slag. Researchers believe that using 60% copper slag instead of ordinary sand might improve or maintain the long-term durability of SCC [10]. Najimi et al. [11] Expansion measurements, compressive strength degradation, and microstructure studies were performed in sulphate solution on concretes prepared with 0%, 5%, 10%, and 15% copper slag waste. This research suggests copper slag as a sulphate-resistant concrete substitute [11]. Mithun and Narasimhan [12] results demonstrate that AASC/CS mixtures may substitute sand up to 100% (by volume) with no discernible reduction in strength [12]. Brindha and Nagan [13] an M20-grade concrete was employed as a control in this study to compare the results. Increases in free water content in the mix result in lower compressive strength for larger percentage replacement levels of copper slag in cement (more than 20%) and in aggregate (greater than 50%) [13]. Chithra et al. [14]. Because nanosilica has a large specific surface area, it requires a lot of water. Colloidal nanosilica was shown to be an excellent filler and activator for pozzolanic activity. With a 2% nanosilica replacement level, the strength qualities are improved [14]. Sandra et al. [15] the results show that CUS substitution does not affect the mineral composition of the studied concrete mixes, indicating that it may be used with OPC blends. Adding copper slag fine aggregate to concrete as a way to dispose of industrial waste offers a wide variety of construction uses [15]. The behaviour of waste copper slag-based self-compacting concrete (SCC) must be evaluated according to the current literature. To bridge this gap, Waste copper slag is substituted for sand at 0%, 10%, 20%, 30%, 40%, 50%, 60%, and 70% in this study. SCC-WCS% was tested for compressive strength, bond stress, and durability tests of water absorption, sorptivity, and rapid chloride permeability were tested. Statically analysis is conducted on CMS with durability properties of SCC-WCS% mixes. The SCC-WCS% properties were determined using an XRD technique, and scanning electron microscopy (SEM) and energy-dispersive spectroscopy (EDS) morphology was found at 28 days of curing.

2 Experimental program

2.1 Materials

IS 269-2015 [16] specifies the OPC 53 grade for use in this study. Fly ash (FA) was supplied by VTPS in Andhra Pradesh, India. Tables 1 and 2 list the chemical and physical parameters of materials. Fine and coarse aggregates (diameters 10–12.5 mm) are gathered from the nearby area for the study. IS 9103: 1999 [17] calls for determining SCC-WCS percent combination characteristics in the lab using tap water and a 1.09-specific gravity HRWR.

Table 1 Chemical properties of materials for SCC-WCS mix

Chemical composition	Cao	K_2O	Na_2O	MgO	Al_2O_3	SO_3	SiO_2	FeO
WCS (%)	0.05	0.3	0.6	1	3	0.1	28	45
Flyash (%)	1.3	1.98	1.1	1.54	27.4	0.05	58.5	5.1
Cement (%)	63.6	0.45	0.22	0.8	4.8	2.2	21.9	3.9

Table 2 Physical properties of materials for SCC-WCS mix

Physical properties	WCS	Natural sand	Cement	Coarse aggregate	Standard codes for testing
Fineness modulus	3.32	2.61		6.1	IS: 383-2016 [18]
Specificdensity (kg/cu.m)	3150	2520	3150	2489	IS:2386 (Part-III)-1963 [19]
Bulk density (kg/cu.m)	3250	1658		1503	IS: 383-2016 [18]
Water absorption (%)	0.14	2.8	–	–	IS:383-2016 [18], IS:2386 (Part-III)-1963 [19]

2.2 Mix proportion

A total of eight mixes, including a control mix, were prepared. Natural sand is replaced with WCS, which may vary from 0 to 70% in SCC. The ideal SCC mix ratio: 425 kg/m^3 cement, 92.35 kg/m^3 flash, 904 kg/m^3 coarse-grain-crushed aggregates, 740 kg/m^3 natural sand, 0.43 water to cement and PCE superplasticizer at 4.17 kg/m^3 and tap water are used to mix for preparation. It takes around 8–10 min in a pan mixer to get a uniform mixture. EFNARC [20, 21], IS 10262: 2019 [22] and ACI-237R-07 [23] all state that flow qualities should be evaluated.

3 Research methodology

The entire research methodology is represented in a graphical form chart shown in Fig. 1. The various tests conducted and the methodology is discussed as follows:

3.1 Mechanical strength

To assess the strength of the SCC-WCS% cube, samples are removed from the moulds and curing is done for 28 and 56 days until they are ready for testing in the lab. Compressive strength tests (CMS) are performed on 100 × 100 × 100 mm cube specimens made in the lab under IS 516:2015 [24]. For testing cubes, 100 tones of UTM of capacity are used for the study.

3.2 Bond stress

Prism specimens with dimensions of 100 × 100 × 100 mm were prepared for pull-out experiments as per IS: 2770 (Part I)—1967 [25]. In this experiment, the diameter of the deformed reinforcing bar was 12 mm, and the overall length was 900 mm are prepared as shown in Fig. 2. Bond stress between the SCC-WCS% mix samples to rebar pull-out test is conducted. The bond stress is the ratio of maximum pull-out force to the bonded area of the rebar. To calculate the bond stress is represented in Eq. 1.

$$\tau = \frac{\text{Pmax}}{\pi DLd}, \tag{1}$$

Fig. 2 Samples prepared for the pull-out test

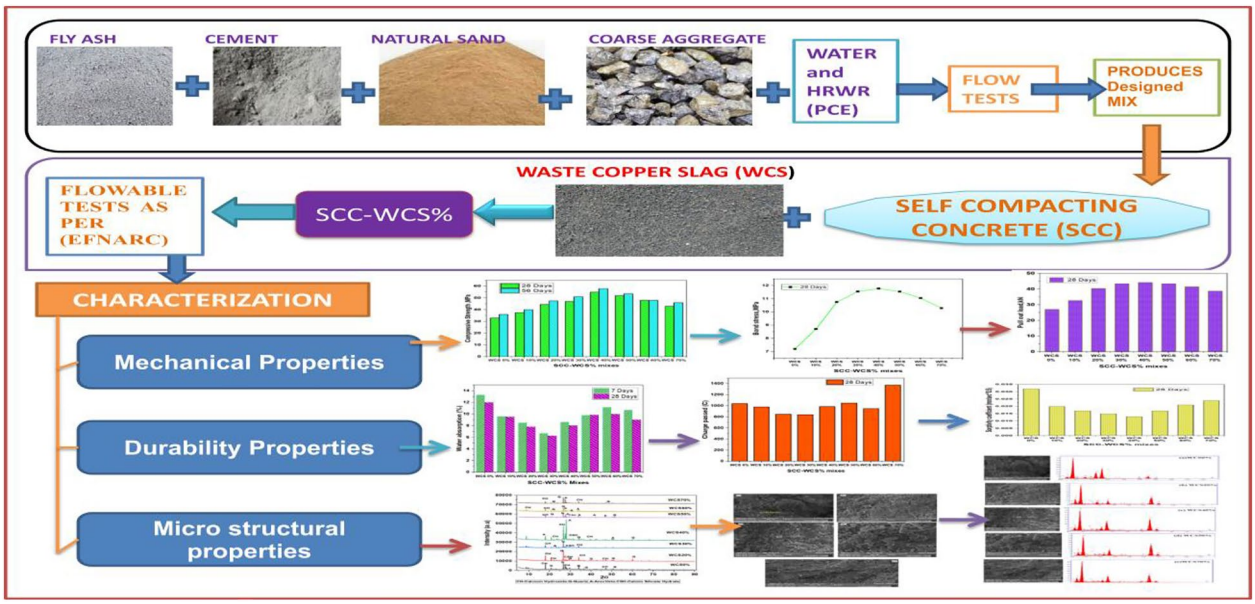

Fig. 1 Graphical chart of research methodology of SCC-WCS% mixes

where P max is the maximum pull-out load (N), d_b is the effective diameter (mm), and L_d is the embedded length.

3.3 Durability tests

3.3.1 Water absorption

All concrete samples have been subjected to a water absorption test following IS 1124-1974 [26]. For testing, samples were kept at 105 °C in an oven to ensure that no moisture was present within the concrete. From Eq. (2), we can assess the water absorption of SCC-WCS% samples after 28 days of curing.

Wa = saturated sample wt (g) after 24 h of soaking, Wd = dry weight of the sample at room temperature.

$$\text{Water Absorption}(\%) = \text{W}(\%) = \frac{(Wa - Wd)}{\text{Wd}} \times 100 \qquad (2)$$

3.3.2 Rapid chloride penetration test

To know the chloride penetration of SCC with the incorporation of WCS from 0 to 70% (10% increment). A rapid chloride penetration test (RCPT) was conducted as per ASTM C1202-12 [27]. For testing the samples, 100 mm ϕ and 50 mm thick cylindrical concrete discs are prepared. Figure 3 illustrates the set for testing chloride penetration for SCC-WCS% mixes. Eight sets are prepared in SCC with WCS from 0–70% (10% increment). Each RCPT test set has five cells. As depicted in Fig. 4, each cell has a positive and a negative terminal, and 0.3 M of NaOH and 3% NaCl solutions are used in the study. When measuring the flow of electricity between cells, coulombs are measured. It is possible to determine how much charge travels through the SCC-WCS per cent samples using Eq. 3. The maximum current flow indicates low chloride ionic penetration resistance.

$$Q = 900\left(I_0 + 2I_{30} + 2I_{60} + - - - + 2I_{330} + I_{360}\right), \qquad (3)$$

where Q = Charge passed (Coulombs). I_0, I_{30}, $I_{60...}$ I_{330}, I_{360} = current at 0, 30, 60, ——, 330, 360 min.

3.3.3 Sorptivity test

Water penetration through the SCC-WCS% samples was determined using the sorptivity test according to ASTM C1585-13 [28]. To assess surface water penetration, four models of 100 mm ϕ and 50 mm thick cylindrical concrete discs are prepared in each set after 28 days of curing, and the test is conducted. Eight sets are assessed in SCC with the incorporation of sand with WCS from 0 to 70% (10%

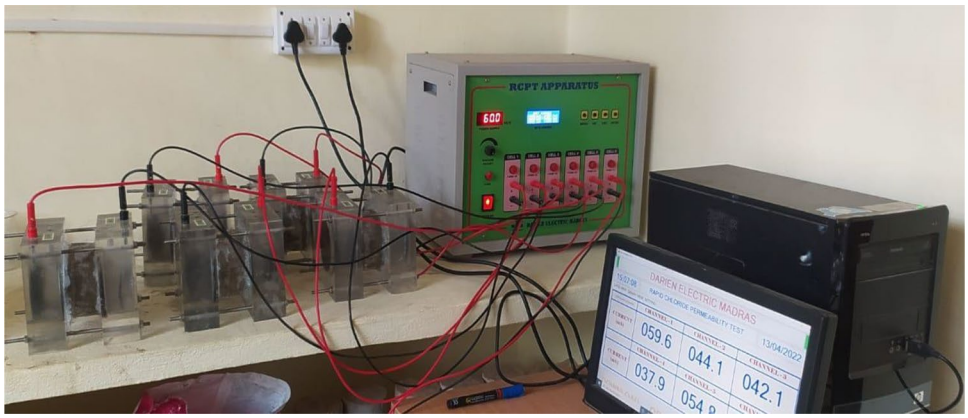

Fig. 3 Set up for RCPT test with cells for SCC-WCS% mixes

Fig. 4 Set up for sorptivity test for SCC-WCS% mixes

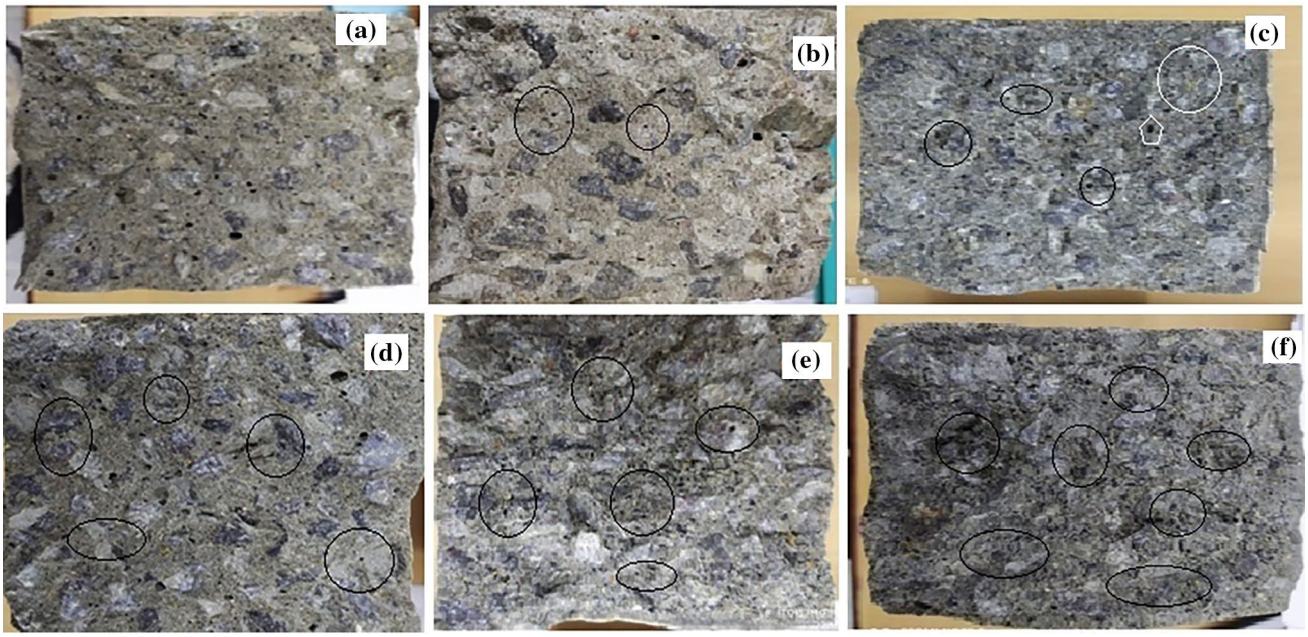

Fig. 5 The cross-sectional view WCS spots in SCC-WCS mixes: **a** WCS 0%, **b** WCS 30%, **c** WCS 40%, **d** WCS 50%, **e** WCS 60%, **f** WCS 70%

increment). The specimens were waxed on all sides except the surface, exposed to water penetration as shown in Fig. 4, and the sorptivity values were computed using Eq. (4).

$$S = \frac{i}{\sqrt{t}} \tag{4}$$

S = coeff. of sorptivity (mm/min 0.5), i = cumulative water absorption and t = time (min),

3.4 Microstructure analysis

The sample's crystalline structure and morphology must be studied using microstructure analysis. SCC-WCS per cent mix samples were analyzed at 28 days of curing for XRD and SEM in this investigation. In addition, XRD analysis was carried out on powder samples of SCC mixtures that heat-treated and ambient. The SEM, VEG3, and SBHTES-CAN are utilized at 15 kN (or) 10 kN to explore backscattered electron imaging.

4 Results and discussion

4.1 Compressive strength (CMS)

The CMS values of the SCC-WCS% mix at 28 and 56 days are represented in Fig. 6. SCC with WCS as sand substitute represents an incremental trend in CMS compared to the control concrete (SCC-WCS0%) at 28, 56 days of curing.

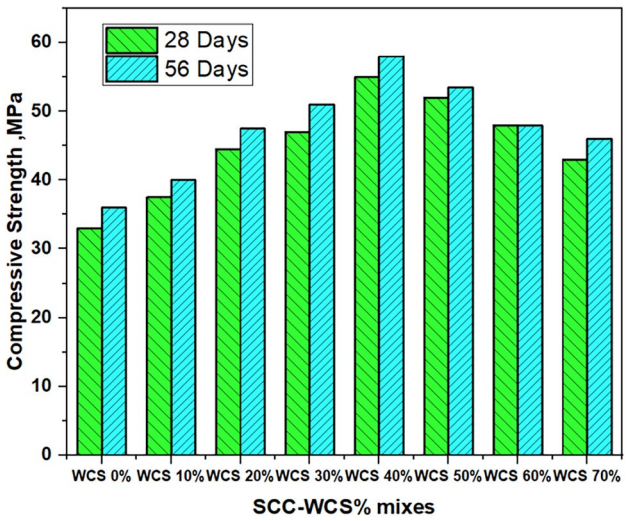

Fig. 6 CMS for SCC-WCS% mixes

SCC samples made up of 70% WCS showed better compressive strength than those of 0% WCS. Incorporating WCS into SCC as a sand substitute significantly improved its strength at 28 and 56 days. At 28 and 56 days,SCC having 10, 20, 30,40,50,60 and 70% of WCS as sand has attained 13.63, 34, 42, 23,57,45,30% and 11.11, 31.94, 41.66, 22.1, 48.6, 33.33,27.77% greater to the pure sand-based SCC sample (SCC-WCS0%) in terms of strength. The w/c of 0.43 provides a homogeneous mix with high workability in the SCC-WCS mix, which improves strength. Chemical reactions involving reactive silica and alkali calcium

hydroxide produce calcium silicate and aluminates, which are then formed in the cement paste. Enhanced compressive strength is achieved by the chemical interaction of ITZ with calcium silicate and aluminium oxide hydrates [29–33]. Copper slag's high density and texture are further factors [5, 34–38]. Figure 5 illustrates the SCC samples containing 0%, 30%, 40%, 50%, 60% and 70% WCS spots. By substituting copper slag with sand from 0 to 100% concrete at w/c ratios of 0.45 and 0.55, the maximum strength values of 50.2, 48.2, and 50.2 MPa were achieved when using 20–60% of the CS, compared to 0% in traditional concrete [35]. There was a reported increase in stress in self-compacting concrete of up to 30% with sand replacement [38] and up to 20% with cement substitution at 28 days of curing the concrete because of the high cost of cement and environmental protection [3, 39].

4.2 Bond stress

The bond behaviour between concrete and rebar pull-out test is conducted [40–44]. In SCC with replacement of sand with WCS from 0 to 70% for that bond behaviour and stress of SCC-WCS% with rebars are observed. Figures 7 and 8 represents the experimental data of pull-out load and bond stress of SCC-WCS% mixes at 28 days. Using the WCS content, the bond stress and pull-out values are increased compared to the control concrete (SCC-WCS0%). The maximum pull-out load range between 27.12 to 44.35 kN and the bond strength range from 7.198 to 11.766 MPa are shown in Figs. 7 and 8. At 28 days curing bond stress, SCC having 10, 20, 30, 40, 50, 60 and 70% of WCS as sand has attained 20.86%, 49.34%, 60.50%, 63.46%, 60.32%, 53.50% and 42.86% compare to the control concrete (SCC-WCS0%) as shown in Fig. 8. The bond stress values of SCC replacement with WCS from 10 to 70% show more resistance in strength compare to IS:456:2000 [45].

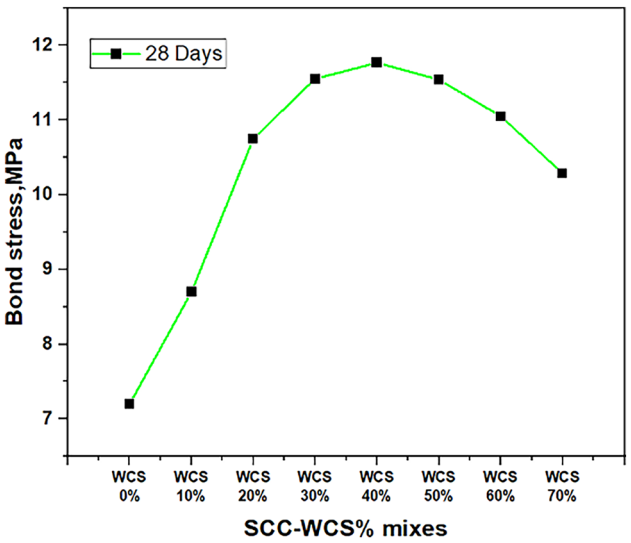

Fig. 8 Bond stress for SCC-WCS% mixes

4.3 Water absorption

Figure 9 depict the water absorption of SCC-WCS% at 7 and 28 days of curing. SCC mixes incorporating WCS% content as sand show a reduction in the water absorption values up to WCS50% and a slight increase at WCS 60% and WCS 70% both at 7 days and 28 days of curing. The SCC mixes with 0,10, 20, 30, 40, 50% of WCS mixes have

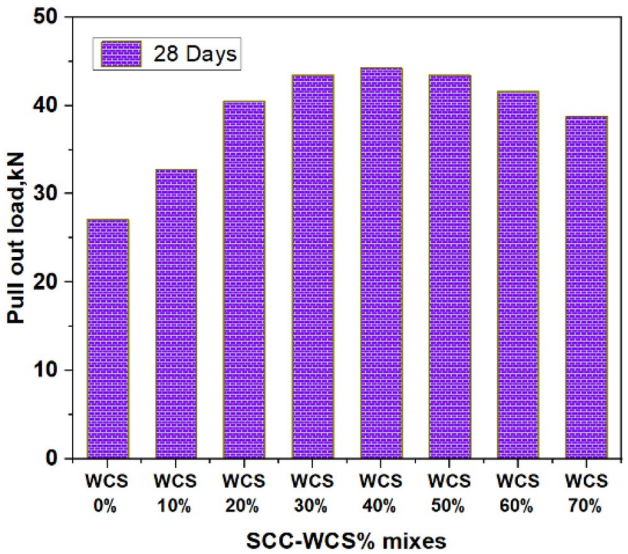

Fig. 7 Pull-out load for SCC-WCS% mixes

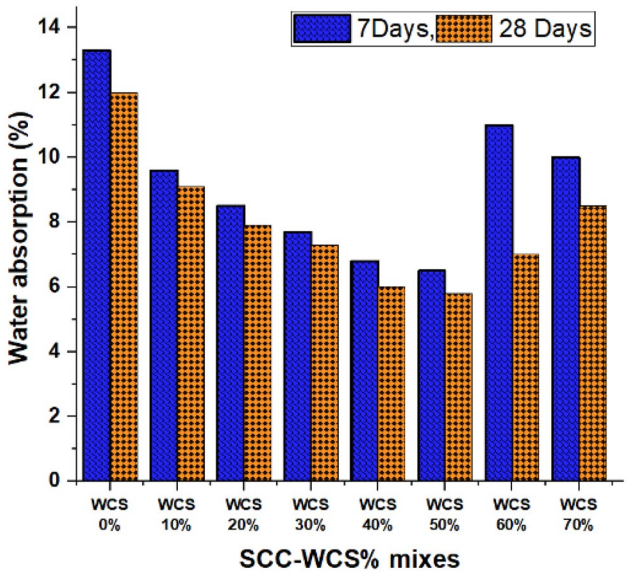

Fig. 9 Water absorption (%) for SCC-WCS% mixes

shown 13.33%, 9.6%, 8.5%, 7.69%, 6.8%, 6.5% and 13%, 9.1%, 7.9%, 7.3%, 6%, 5.8% water absorption rate compare to control concrete (SCC-WCS 0%) at 7 days and 28 days of curing period.WCS percent has a low water absorption rate, resulting in the production of a denser structure with fly ash [1, 2, 8, 37]. The concrete's water absorption value improved somewhat at WCS 60% and WCS 70% when copper slag was used. When copper slag percentages were increased in SCC combinations, the free water content increased, resulting in more voids. The increase in water absorption rate is negligible compared to SCC mixes with 100% sand. For 28 days, the water absorption rate in WCS 100% sand (WCS0%) is 13%,in WCS 60% and 70%, the rates are 7% and 8.5%. This might be owing to the reduced surface absorption of waste copper slag particles compared to sand, which could lead to an increase in water absorption.

4.4 Rapid chloride permeability test

SCC chloride ion permeability was measured using RCPT with sand replacement WCS ranging from 0 to 70%. (10% increment). Table 4 shows the RCPT, standards as per the following ASTM C 1202-07 [27]. Table 3 displays the results of the RCPT SCC-WCS percent sample. Figure 10 indicates a decrease in chloride ion permeability with WCS replacements for fine aggregates. The higher chloride ion penetration was observed for WCS 70% samples in term charge passed 1090 coulombs. SCC mixes including up to 40% copper slag showed a substantial reduction in RCPT after 28 days. By reducing pores, copper slag reduced concrete's permeability [9]. Adding WCS reduced water absorption by up to 50%, according to the experiment results. All SCC mixes had low chloride permeability at 28 days. The coulombs ranged from 880 to 1340 FA and WCS percent mixes of SCC exhibited better chloride ion combat than other SCC-100% sand blends in Fig. 10. The addition of particles such as fly ash and copper slag may have increased the matrix's particle packing density, reducing chloride ion penetration. Chloride iron penetration in Self Compacting Concrete was greatly decreased as a result of the addition of Flyash and WCS to the microstructure and improved pore structure. A decrease in RCPT values was seen in a fly ash-based geo polymer mortar with nanosilica additions [32] because the mixture included more crystalline components. Slag admixed concrete has been rated "extremely poor" in terms of its quality. As a result, it suggests that slag additive concrete has a lower permeability. The slag minimizes the pores in the concrete and makes the concrete impermeable [13].

Table 3 Chloride ion permeability values for SCC-WCS% mixes

SCC-Mix ID	Current passed (C) 28 days	Chloride ion permeability (ASTM C1202-07) [27]
SCC-WCS 0%	1340	Low
SCC-WCS 10%	1180	Low
SCC-WCS 20%	1050	Very low
SCC-WCS 30%	950	Very low
SCC-WCS 40%	880	Very low
SCC-WCS 50%	950	Very low
SCC-WCS 60%	1030	Low
SCC-WCS 70%	1090	Low

Table 4 Chloride ion permeability as per standards

S. no	1	2	3	4	5
Charge passed (C)	> 4000	2000–4000	1000–2000	100–1000	< 100
(ASTM C 1202-07) Chloride ion permeability [27]	High	Moderate	Low	Very low	Negligible

4.5 Sorptivity test

Sorptivity's endurance is connected to water absorption through capillary pores in the microstructure. Capillary pores in the microstructure of concrete are primarily responsible for concrete's adsorption capacities. When the volume of capillary holes is greater, the sorptivity is bigger, and the likelihood of concrete degradation increases [10]. At 28 days

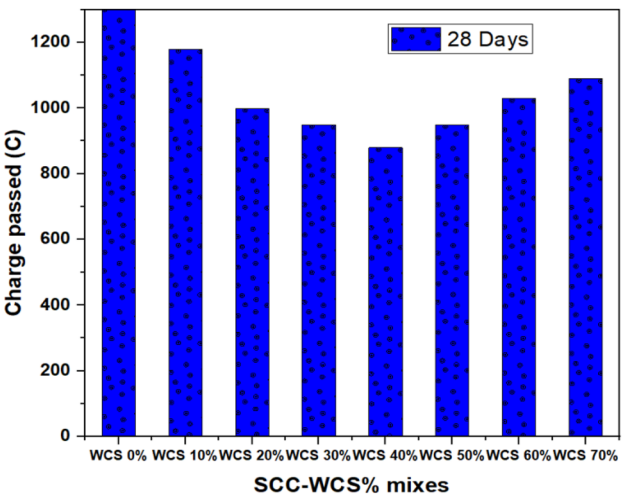

Fig. 10 Charge passage of coulombs for SCC-WCS% mixes

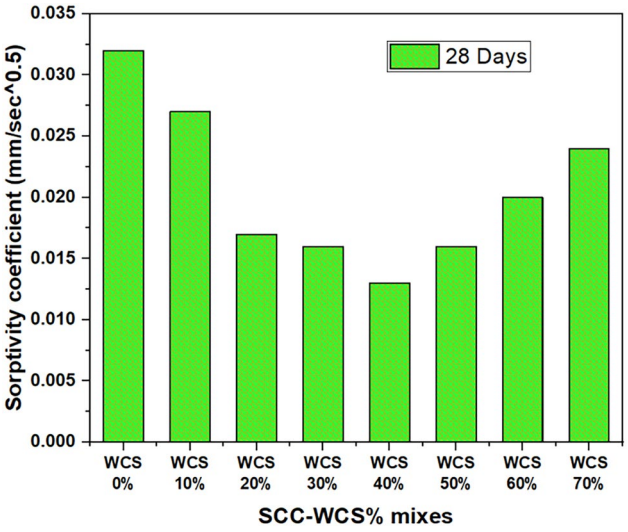

Fig. 11 Sorptivity values of SCC-WCS% mix samples

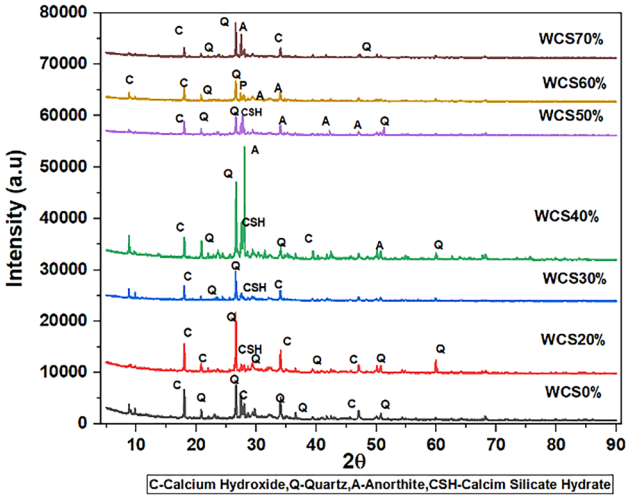

Fig. 12 Xrd peaks of SCC-WCS% mix samples

of curing age, about 30%, 39.23%, 43.84%, 53.84%, 55.38%, 46.15% and 34.64 % of decrease was observed in the water absorption corresponding to WCS10%, WCS20%, WCS30%, WCS40%, WCS50%, WCS60% and WCS70% with respect to control concrete (WCS0%) represents in Fig. 11. Concrete with a sorptivity of SCC-WCS0 percent i.e. 0.032 mm/min$^{0.5}$ sorptivity for 28 days For SCC-WCS10% to SCC-WCS70%, the lowest values of sorptivity were 0.02, 0.017, 0.015, 0.013, 0.017, 0.021, and 0.029 mm/min$^{0.5}$ at 28-day curing age, respectively. Compared to control concrete, surface water absorption decreased 37.5, 46.8, 53.1, 59.3, 46, 8, 34, and 25% after 28 days of curing age (SCC-WCS0%). Capillary pores in the microstructure are discussed in sorptivity and water absorption whereas water absorption at the concrete surface under a gradient of pressure head is established. To understand how SCC mixtures perform, it is important to understand how void volume and pore microstructure affect the mix's durability. Water absorption and sorptivity were shown to increase after WCS60% and WCS70%. There was a decrease in durability up to WCS50% due to reduced water absorption qualities and WCS's larger grain size than natural sand, which increased voids, capillary channels and interfacial transition zone thickness [10].

4.6 X-ray diffraction

X-ray diffraction (XRD) techniques was evaluated on phase are tested in the hardened SCC matrix with sand replacement of WCS% from 0%, 10%, 20%, 30%, 40%, 50%, 60% and 70%. For XRD investigation, powder samples were taken from each SCC-WCS per cent combination after 28 days of curing. We utilized 2θ that spanned from 5° to 90° to conduct XRD analysis. Figure 12 Xrd peaks of SCC-WCS% mix samples. The multi-peaks in the SCC-WCS per cent combinations may readily be seen using XRD analysis. Peak phases in SCC combinations include quartz (Q), anorthite (A), calcium hydroxide (C), calcium silicate hydrate (C-S–H), portlandite, and silicon oxide. The main peaks with 2θ at 26.6° of quartz refer to the hexagonal structure. At WCS 40%, the main peak phases of quartz represent crystal structure showing an increment in the strength of SCC mixes other phases C-calcium hydroxide and CSH-calcium silicate hydrate was observed in the SCC mixes [5, 9]. XRD pattern of the SCC-WCS% of mixes of different elements diffraction shows peaks at 2θ value for C is 18.08° and Q is 26.63° which was associated with the hexagonal crystal structures. C–S–H associated with semi-crystalline to normal amorphous structure shows peaks of 2θ value is 27.99° and A-anorthite associated with triclinic crystal shows peaks of 2θ value is 27.5°. Table 5 represents the Xrd diffraction characterizes SCC-WCS% mixes.

4.7 SEM/EDS analysis

SEM/EDS analysis is done for SCC-WCS% mixtures of the concrete matrix. The microstructure images of SCC mixes are done at 28 days of curing with WCS% content 0%, 20%, 40%, 50% and 70%. The SEM images at 28 days at magnification range from 1.0 to 4.0Kx are investigated. Figure 13a presented the morphology of SCC with WCS0% leads to the formation of C–S–H layers, ettringite, and voids observed. Figure 13b presents the formation of C–S–H gel and ettringite for SCC-WCS20%, and micro-cracks are observed. As the WCS% content is increased further, shown in Fig. 13c at WCS40% observed denser homogenous C–S–H gel and voids. Accumulation of the C–S–H layer makes the concrete denser, leading to an increment in CMS. Having Si and Ca

Table 5 Xrd peak characterizes SCC-WCS% mixes

S. no.	Mix Id	Element	Phases structure	JCPDS number
1	WCS0%	Q-quartz CH-calcium hydroxide	Hexagonal crystal Hexagonal crystal	JCPDS PDF 016-0380
2	WCS10%	Q-quartz CH-calcium hydroxide	Hexagonal crystal Hexagonal crystal	JCPDS PDF 016-0380
3	WCS20%	Q-quartz CH-calcium hydroxide CSH-calcium silicate hydrate	Hexagonal crystal Hexagonal crystal Semi-Crystalline	JCPDS PDF 016-0380 JCPDS CARD 03-0606
4	WCS30%	Q-quartz CH-calcium hydroxide CSH-calcium silicate hydrate	Hexagonal crystal Hexagonal crystal Semi-crystalline	JCPDS PDF 016-0380 JCPDS CARD 03-0606
5	WCS40%	Q-quartz CH-calcium hydroxide CSH-calcium silicate hydrate A-anorthite	Hexagonal crystal Hexagonal crystal Semi-crystalline Triclinic crystal	JCPDS PDF 016-0380 JCPDS CARD 03-0606 JCPDS 89-1472
6	WCS50%	Q-quartz CH-calcium hydroxide CSH-calcium silicate hydrate A-anorthite	Hexagonal crystal Hexagonal crystal Semi-crystalline Triclinic crystal	JCPDS PDF 016-0380 JCPDS CARD 03-0606 JCPDS 89-1472
7	WCS60%	Q-quartz CH-calcium hydroxide A-anorthite	Hexagonal crystal Hexagonal crystal Triclinic crystal	JCPDS PDF 016-0380 JCPDS 89-1472
8	WCS70%	Q-quartz CH-calcium hydroxide A-anorthite	Hexagonal crystal Hexagonal crystal Triclinic crystal	JCPDS PDF 016-0380 JCPDS 89-1472

in the concrete matrix phase results in a dense amount of CSH gel at the IT zone and aluminosilicates gel [35], which increases the mix's strength, and having Fe available in the mixture of 40% of WCS in SCC, but this hasn't shown any effect on the mix's strength characteristics. Figure 13d shows the presence of voids and denser C–S–H layer formation observed at SCC-WCS 50% in the SCC matrix under the SEM image. Figure 13e represents SCC-WCS70% shows voids, micro cracks and C–S–H gel formation in the SEM image.

Figure 13a–e illustrates the SEM images of SCC mixes at replacements sand with WCS% from 0%, 20%, 40%, 50% and 70%. All replacement levels resulted in denser and more homogeneous concrete mixtures [9]. Ettringite and voids were detected in SCC mixtures including more than 50% copper slag in place of sand. Improvements in the CMS of the SCC matrix are observed from SEM images of denser and homogenous C-S–H gel formation in the concrete matrix with all the replacements of sand with WCS compared to the control concrete (without WCS) [35, 36, 38, 46].

In EDS analysis, Fig. 14a shows that Al, Si, Ca, C and O lead to ettringite formation under EDS analysis. Figure 14b represents Ca, Si, S and O peaks observed in the EDS analysis of SCC-WCS20%. Figure 14c represents the major peaks of Si, Ca, Al, S, C and O; observed these elements lead to the formation of denser C–S–H gel in the concrete matrix; it is seen in SEM image Fig. 13c. Figure 14d illustrates dense C–S–H gel formation and voids, but CMS is more than the control concrete (SCC-WCS 0%). The major peaks of Al, S, Ca, C and O are observed, leads the formation of the C–S–H layer in EDS analysis in Fig. 14d. Figure 14e shows S, Al, Ca and O peaks in WCS70% in the SCC matrix. Figure 14a–e showed the elemental composition of SCC-WCS% from EDS analysis with peaks present, Al, Si, Ca, and C indicates the increment in the CMS with the incorporation of WCS%.

5 Statistical analysis

Compressive strength and RCPT (charge passed) values, water absorption, and sorptivity of SCC mixtures containing copper slag were studied using linear regression analysis for values up to 28 days of curing. Figure 15 shows the correlation coefficient (R^2) of 0.882 between CMS and water absorption. Figure 16 shows a relationship between compressive strength and RCPT values. Compressive strength was found to have a correlation coefficient of 0.908% with the RCPT values (Fig. 16). Water absorption, chloride ion permeability, and sorptivity, all of which are indicators of long-term durability, decrease with increasing strength. This added credence to the testing results for strength and durability. The analysis of the connections between several durability qualities revealed the interdependence of their effects.

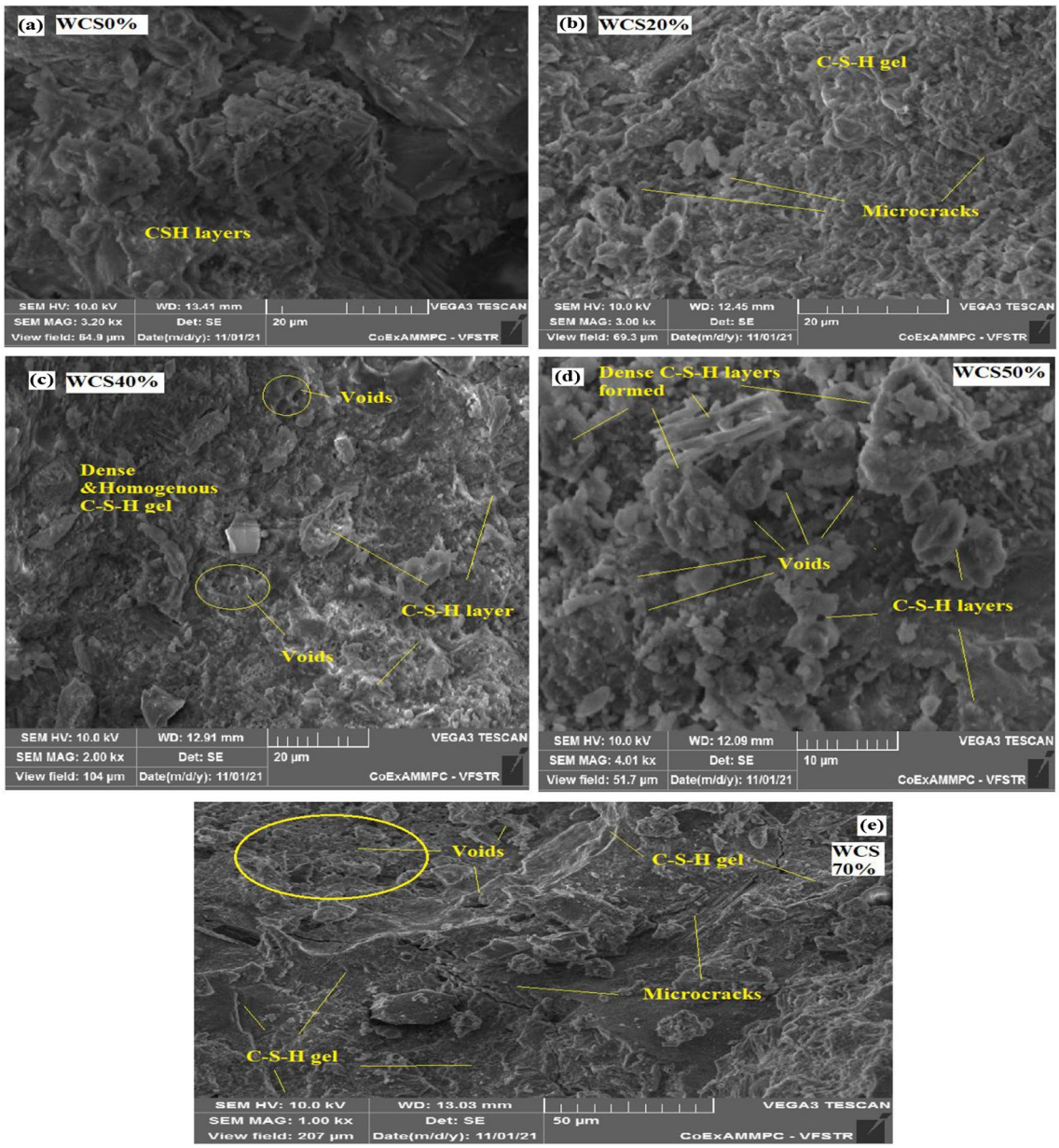

Fig. 13 **a–e** SEM image of SCC-WCS% mix samples

Figure 17 shows that the sorptivity of CMS and the charge passed in SCC mixes are closely connected with coefficients of 0.996 and 0.896, respectively. In Fig. 18. Linear regression analysis demonstrates a correlation coefficient of 0.905 and 0.84 between the water absorption of SCC mixes and the RCPT (charge passed) values and sorptivity during 28 days. Water absorption was decreased due to a reduction in the number of pores and gaps in the concrete matrix. Incorporating WCS and fly ash may lower the system's chloride-ion permeability. Increasing the porosity of SCC results in an increase in its strength properties [9, 47].

6 Conclusion

The objective of the present research is to study the behavior of SCC with copper slag waste as a secondary source of fine aggregates from 0 to 70% in the mixes for ensuring a sustainable environment. The parameters are bond behaviour,

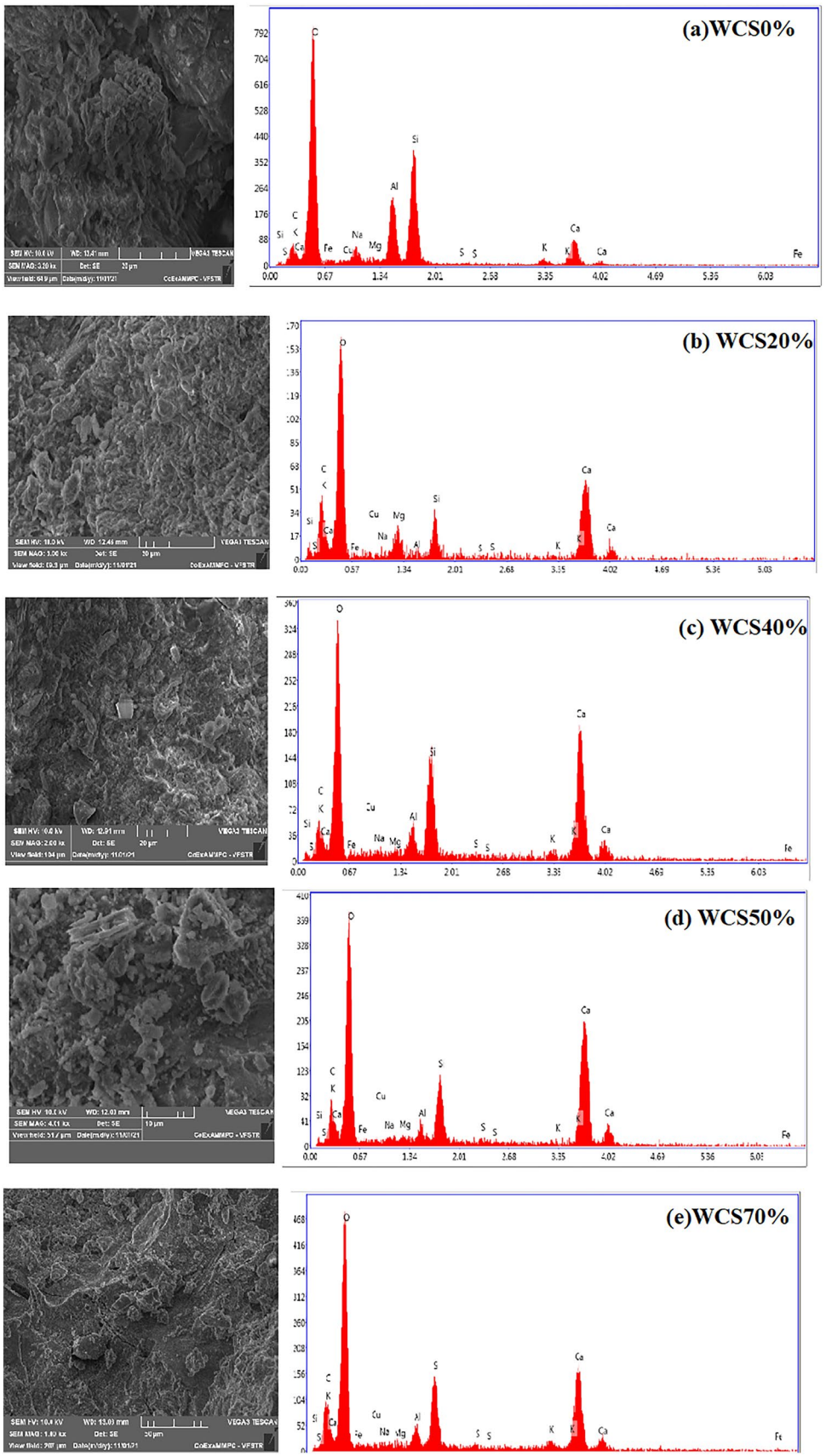

Fig. 14 **a**–**e** EDS analysis of SCC-WCS% mix samples

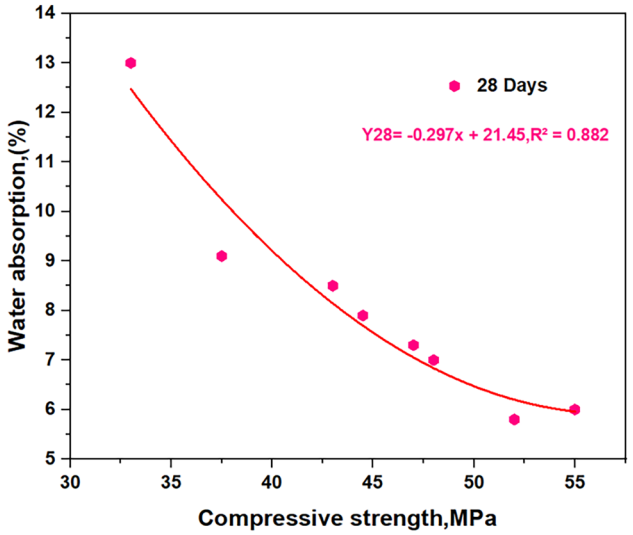

Fig. 15 Correlation of CMS vs water absorption in SCC-WCS% mixes

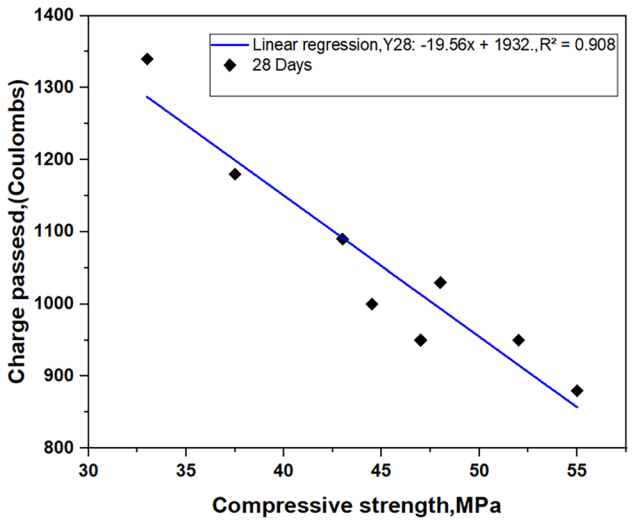

Fig. 16 Correlation of CMS vs charge passed (RCPT) in SCC-WCS% mixes

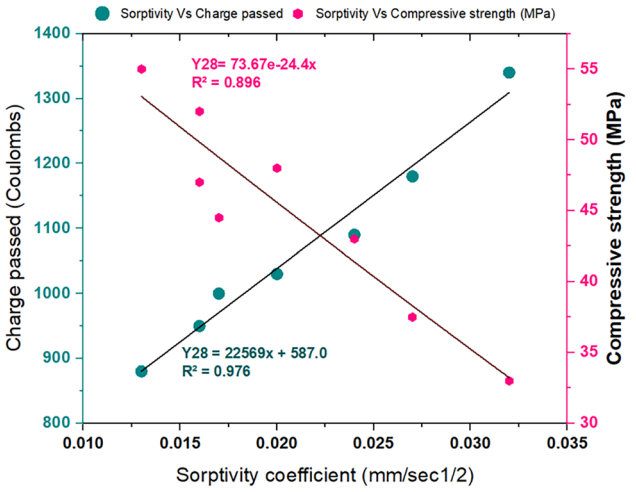

Fig. 17 Correlation of sorptivity coefficient vs CMS and charge passed in SCC-WCS%

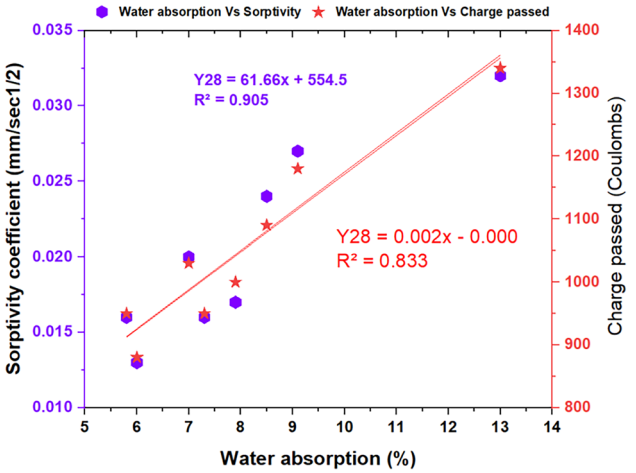

Fig. 18 Correlation of water absorption vs sorptivity and charge passed in SCC-WCS%

mechanical, durability and microstructural properties of concrete carried out in this research.

These conclusions can be drawn as a result of this investigation:

1. Having a more significant amount of silica hastened the CMS improvement. Due to this, WCS achieves peak strength at an earlier age than conventional concrete. The compressive strength of SCC-WCS, which substitutes WCS for 40% of the sand, has improved.
2. When copper slag was used to replace up to half of the SCC, the water absorption was significantly decreased. With 40%, and 50% WCS, the absorption rate dropped by 6.8%, by 6%, and by 6.5, 5.8% at 7, 28 days of age. Due to WCS's lower water absorption and varied gradation, voids, capillary channels, and interfacial transition zone thickness were increased.
3. The sorptivity of SCC mixtures including copper slag reduced after 28 days. After 28 days, decreases of about 47%, 50%, 59%, 50%, and 37.5% were recorded at slag replacement rates ranging from 20 to 60%. Although the maximum sorptivity values decreased by 59% at a WCS concentration of 40%, they remained higher than the control concrete (WCS 0%).
4. In the SCC-WCS% samples, the chloride permeability is very low up to 40% WCS content at 70%WCS is low. Due to its low value, the primary causes of steel cor-

rosion in reinforced concrete structures surface passive layer is more effectively used as a sand replacement up to 40% in SCC.

5. SEM/EDS and XRD studies demonstrated that C–S–H production filled all of the capillary layers and produced thick concrete with all of the microcracks and holes present in dense structures. In addition, due to a solid pozzolanic reaction and SCC-WCS percentage of 40% to 50%, the SCC mix was effective compared to the control concrete.
6. CMS and durability characteristics showed good statistical connections with water absorption, sorptivity values, charge passed (RCPT) of SCC validating the results obtained.

This study suggests up to 70% is used as WCS substitution with sand compared to control concrete for the development of SCC due to better durability properties. The past researchers have recommended the optimal content of 40% as fine aggregates for normal vibrated concrete and high-performance concrete and 20% for SCC.

Funding No.

Code availability Not applicable.

Declarations

Conflict of interest The author declared there is no conflict of interest on behalf of all authors.

References

1. Rajasekar A, Arunachalam K, Kottaisamy M (2019) Assessment of strength and durability characteristics of copper slag incorporated ultra-high strength concrete. J Clean Prod 208:402–414
2. Dey S, Kumar VVP, Goud KR et al (2021) State of art review on self-compacting concrete using mineral admixtures. J Build Rehabil 6:18. https://doi.org/10.1007/s41024-021-00110-9
3. Hooton R, Al-Jabri K, Taha R, Al-Ghassani M (2002) Use of copper slag and cement by-pass dust as cementitious materials. Cement Concr Aggreg 24(1):7
4. Samabangi A, Eluru A (2022) Industrial copper waste as a sustainable material in high strength SCC. Clean Eng Technol 6:100403
5. Chaitanya BK, Sivakumar I (2022) Flow-behaviour, microstructure, and strength properties of self-compacting concrete using waste copper slag as fine aggregate. Innov Infrastruct Solut 7:181. https://doi.org/10.1007/s41062-022-00766-3
6. Chaitanya BK, Kumar IS (2022) Effect of waste copper slag as a substitute in cement and concrete—a review. IOP Conf Ser Earth Environ Sci 982(1):012029. https://doi.org/10.1088/1755-1315/982/1/012029
7. Krishna Chaitanya B, Sivakumar I (2021) Influence of waste copper slag on flexural strength properties of self-compacting concrete. Mater Today Proc 42:671–676
8. Sharma R, Khan RA (2018) Influence of copper slag and metakaolin on the durability of self-compacting concrete. J Clean Prod 171:1171–1186
9. Gupta N, Siddique R (2020) Durability characteristics of self-compacting concrete made with copper slag. Constr Build Mater 247:118580. https://doi.org/10.1016/j.conbuildmat.2020.118580
10. Sharma R, Khan RA (2017) Durability assessment of self compacting concrete incorporating copper slag as fine aggregates. Constr Build Mater 155:617–629. https://doi.org/10.1016/j.conbuildmat.2017.08.074
11. Najimi M, Sobhani J, Pourkhorshidi A (2011) Durability of copper slag contained concrete exposed to sulfate attack. Constr Build Mater 25(4):1895–1905. https://doi.org/10.1016/j.conbuildmat.2010.11.067
12. Mithun BM, Narasimhan MC (2016) Performance of alkali activated slag concrete mixes incorporating copper slag as fine aggregate. J Clean Prod 112(1):837–844. https://doi.org/10.1016/j.jclepro.2015.06.026
13. Brindha D, Nagan S (2011) Durability studies on copper clag admixed concrete. Asian J Civ Eng (Build Hous) 12(5):563–578
14. Chithra S, Senthil Kumar S, Chinnaraju K (2016) The effect of colloidal nano-silica on workability, mechanical and durability properties of high-performance concrete with copper slag as partial fine aggregate. Constr Build Mater 113:794–804
15. Sandra N, Kawaai K, Ujike I (2020) Influence of copper slag on corrosion behavior of horizontal steel bars in reinforced concrete column specimen due to chloride-induced corrosion. Constr Build Mater 255:119265
16. IS:269:2015 (2015) Ordinary portland cement—specification (sixth revision). Bureau of Indian Standard, New Delhi
17. IS 9103: 1999 (1999) Concrete admixtures-specification (first revision). Bureau of Indian Standard, New Delhi
18. IS 383-2016 (2016) Specification for coarse and fine aggregates from natural sources for concrete. Bureau Of Indian Standard, New Delhi
19. IS:2386 (Part-3) (1963) Indian Standard methods of test for aggregates for concrete. Bureau of Indian Standard, New Delhi
20. EFNARC (2002) Specification and guidelines for self-compacting concrete
21. EFNARC (2005) The European guidelines for self-compacting concrete. Specification, Production and Use
22. IS 10262:2019, Concrete mix, proportioning guidelines (first revision). Bureau of Indian Standard, New Delhi
23. ACI-237R-07 (2007) Self-consolidating concrete. ACI Committee 237, USA
24. IS 516:2015 (2015) Methods of tests for strength of concrete. Bureau of Indian Standard, New Delhi
25. IS 2770 (Part I)—1967 (Reaffirmed 2007) (2007) Indian Standard methods of testing bond in reinforced concrete (part 1): pull-out test
26. BIS, IS 1124-1974 (1974) Specification for water absorption for concrete. Bureau of Indian Standards, New Delhi
27. ASTM C1202-07 (2007) Standard test method for electrical indication of concrete's ability to resist chloride ion penetration. ASTM International, West Conshohocken
28. ASTM C1585-13 (2013) Standard test method for measurement of rate of absorption of water by hydraulic-cement concretes. ASTM International, West Conshohocken
29. Arel HS, Aydin E (2018) Use of industrial and agricultural wastes in construction concrete. ACI Mater J. https://doi.org/10.14359/51700991
30. Aydin E, Arel HŞ (2017) Characterization of high-volume fly-ash cement pastes for sustainable construction applications. Constr Build Mater 157:96–107 (**ISSN 0950-0618**)
31. Jalal M, Mansouri E, Sharifipour M, Pouladkhan AR (2012) Mechanical, rheological, durability and microstructural properties

of high-performance self-compacting concrete containing SiO_2 micro and nanoparticles. Mater Des 34:389–400
32. Adak D, Sarkar M, Mandal S (2014) Effect of nano-silica on strength and durability of fly ash based geopolymer mortar. Constr Build Mater 70:453–459
33. Dey S, Kumar VVP, Manoj AV (2022) An experimental study on strength and durability characteristics of self-curing self-compacting concrete. Struct Concr. https://doi.org/10.1002/suco.202100446
34. Mavroulidou M (2017) Mechanical properties and durability of concrete with water-cooled copper slag aggregate. Waste Biomass Valoriz 8(5):1841–1854
35. Sharifi Y, Afshoon I, Asad-Abadi S, Aslani F (2020) Environmental protection by using waste copper slag as a coarse aggregate in self-compacting concrete. J Environ Manag 271:111013
36. Swathi V, Asadi SS (2022) An experimental investigation on mechanical, durability and microstructural properties of high-volume fly ash-based concrete. J Build Pathol Rehabil. https://doi.org/10.1007/s41024-022-00172-3
37. Venkatesh C, Ruben N, Madduru SR (2020) Role of red mud as a cementing material in concrete: a comprehensive study on durability behavior. Innov Infrastruct Solut 6:13. https://doi.org/10.1007/s41062-020-00371-2
38. Gupta N, Siddique R (2019) Strength and micro-structural properties of self-compacting concrete incorporating copper slag. Constr Build Mater 224:894–908
39. Fadaee M, Mirhosseini RT, Tabatabaei R, Fadaee M (2015) Investigation on using copper slag as part of cementitious materials in self compacting concrete. Asian J Civ Eng (BHRC) 16(3):368–381
40. Nurwidayati R, Ekaputri J, Triwulan T, Suprobo P (2019) Bond behaviour between reinforcing bars and geopolymer concrete by using pull-out test. MATEC Web Conf 280:04008. https://doi.org/10.1051/matecconf/201928004008
41. Baena M, Torres L, Turon A, Barris C (2009) Experimental study of bond behaviour between concrete and FRP bars using a pull-out test. Compos Part B Eng 40(8):784–797
42. de Almeida Filho FM, El Debs MK, El Debs ALHC (2008) Bond-slip behavior of self-compacting concrete and vibrated concrete using pull-out and beam tests. Mater Struct 41:1073–1089. https://doi.org/10.1617/s11527-007-9307-0
43. Ponmalar P (2018) Bond behaviour of self-compacting concrete. Sel Sci Pap J Civ Eng 13:95–105. https://doi.org/10.1515/sspjce-2018-0009
44. Cunha VMCF, Barros JAO, Sena-Cruz JM (2010) Pull-out behavior of steel fibers in self-compacting concrete. J Mater Civ Eng 22(1):1–9. https://doi.org/10.1061/ASCE_MT.1943-5533.0000001
45. IS 456:2000 (2000) Indian standard plain and reinforced concrete code of practice, (fourth revision). Bureau of Indian Standard, New Delhi
46. Bellum RR, Al Khazaleh M, Pilla RK et al (2022) Effect of slag on strength, durability and microstructural characteristics of fly ash-based geopolymer concrete. J Build Rehabil 7:25. https://doi.org/10.1007/s41024-022-00163-4
47. Khotbehsara MM, Mohseni E, Ozbakkaloglu T, Ranjbar MM (2017) Durability characteristics of self-compacting concrete incorporating pumice and metakaolin. J Mater Civ Eng 29(11):04017218